CHAPTER 3

Brittle Crack Propagation

TERRY ENGELDER

INTRODUCTION

RECENT advances in our understanding of brittle deformation processes have included the definition of geological conditions favouring either crack propagation or shear rupture. *Crack propagation* involves the parting of rock within a narrow process zone with a motion normal to the plane of parting, whereas shear rupture involves a complex network of cracking within intact rock, with the wall rock on either side of the rupture zone simultaneously displaced in shear. The mesoscopic products of crack propagation and shear rupture are *joints* and *shear fractures*, respectively (see discussion of these terms in Chapter 5). Shear fracturing along with reactivation of joints by frictional slip are examples of a general class of brittle process called *faulting*. Much of the early work on brittle deformation processes was influenced by the perception that shear fractures were a very common mode of brittle failure in the upper crust (e.g. Badgley 1965). This perception arose because joints were commonly mistaken for shear fractures (e.g. Bucher 1920, Scheidegger's (1982) discussion of Engelder 1982), particularly if the joints were reactivated in frictional slip.

Early models for earth stress were constrained by the strength of intact rocks under large compressive, differential stresses (e.g. Handin & Hager 1957). Rock strength is the differential stress a rock can sustain without developing a shear fracture. Later, geologists appreciated that an intact rock was not a good model for the upper crust which was cut by pervasive sets of joints and faults. This observation led to the inevitable conclusion that differential stress in the crust was more closely constrained by the frictional strength of pre-existing joints, shear fractures, and faults (e.g. Byerlee 1978, Brace & Kohlstedt 1980). Because the upper crust is so completely pervaded by fractures, differential stress throughout much of the upper crust is regulated by frictional slip and, thus, differential stress remains at a lower level than required to rupture intact rock by shear fracturing. However, this lower differential stress does not preclude crack development which occurs under an effective tensile stress (Etheridge 1983).

An appreciation of the importance of crack propagation in rock arose out of detailed studies of shear fracture development. Although less attention was focused on microcrack development during early work on rock strength, microscopy suggested that crack propagation was an important precursor to shear rupture (Bombolakis & Brace 1963, Scholz 1968). With the certain knowledge that microcrack propagation was an important mechanism leading to faulting of intact rock, theories for shear failure were developed based on the growth of microcracks (McClintock & Walsh 1962). At the same time, field work showed that the formation of joints by crack propagation was a very common mode of failure of intact rock in the crust (Secor 1965, Nickelsen & Hough 1967). During the past decade many of the significant strides in understanding the brittle failure of crustal rocks have come from the analysis of crack propagation using linear elastic fracture mechanics.

A review can capture only the bare essence of our understanding of the cracking processes which has three basic stages: initiation; propagation; and arrest. My review starts with a discussion of the fundamental concepts of *linear elastic fracture mechanics* (LEFM) by focusing on the contributions of Inglis, Griffith, and Irwin. Then I discuss the basics of crack initiation using a couple of examples of crack propagation under the influence of high fluid pressure. Such examples are appropriate because one of the most appealing mechanisms for crack propagation deep in the crust is the fluid drive mechanism which acts to relieve high fluid pressure. However, the rules of fracture mechanics developed for fluid-driven cracks apply to all situations involving crack propagation such as those associated with near-surfce jointing where net tensile stresses develop (e.g. Hancock & Engelder 1989). Because of space limits, I only touch on the issues associated with crack propagation and arrest which have been covered in books (e.g. Lawn & Wilshaw 1975, Broek 1987, Atkinson 1987, Rossmith 1983) and in review articles (e.g. Anderson & Grew 1977, Atkinson 1984, Pollard & Aydin 1988).

ANALYSES OF CRACKS IN ELASTIC MATERIALS

The study of crack propagation in rock has its origin in the earliest part of the twentieth century. Crack

propagation stems from stress concentrations which develop around holes in elastic materials. Rocks are a composite of grains, matrix, and cement with pore space commonly found at grain boundaries. Large stress concentrations develop around pore space and elastic mismatches between grains and cement when the rock aggregate is subject to boundary tractions (e.g. Gallagher *et al.* 1974). Some of the sharp corners on pore space and inclusions are so oriented that large tensile stresses develop, and it is at these sharp corners that crack propagation initiates.

Inglis' contribution

An understanding of stress concentration in an elastic material is illustrated using a circular hole in an elastic plate. Assume that the circular hole is nowhere near the edge of the plate. If opposite edges of the elastic plate are pulled by a force large enough to cause a tensile stress, σ^r, within the plate, then this remote stress is concentrated three times (i.e. the hoop stress = $3\sigma^r$) at the point (assume that the plate is infinitely thin) on the edge of the circular hole 90° from the direction of the force on the edges of the plate (Fig. 3.1). Tensile stress is negative in sign. Pore space and other stress concentrators in rocks are more likely to be elliptical in cross section. Inglis (1913) introduced a solution for the state of stress in the vicinity of the tip of an elliptical hole with major axis, c, and minor axis, b. In its limiting case, the elliptical hole represents a crack with a very small minor axis, b. If an elastic plate with an elliptical crack is loaded in tension normal to the major axis of the crack, so that stress within the plate far from the crack is σ^r, then the local tensile stress acting at right angles to the major axis of the crack rises to several times that of σ^r. Inglis (1913) found that

$$\sigma^c = \sigma^r \left(1 + 2\frac{c}{b}\right) \tag{1}$$

where σ^c is the stress concentration at the 'crack' tip.

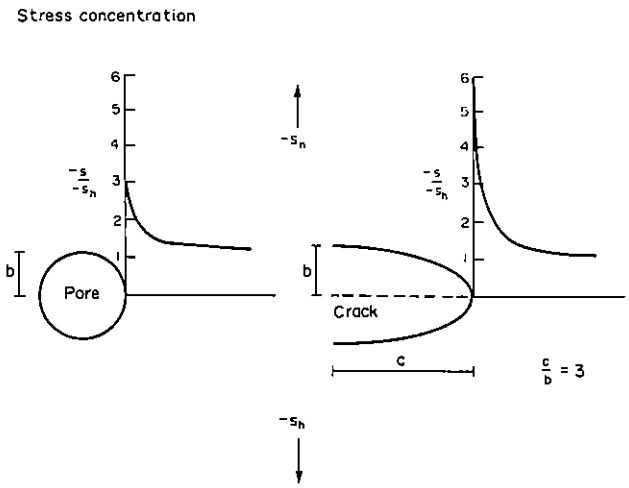

Fig. 3.1. The stress concentration around circular and elliptical holes. See text for details.

The stress concentration decreases rapidly with distance from the edge of the elliptical crack. As the elliptical crack becomes longer with a larger aspect ratio, $\frac{c}{b}$, the stress concentration at the tip of the crack may be approximated by

$$\sigma^c \approx 2\sigma^r \left(\frac{c}{\rho}\right)^{1/2} \tag{2}$$

where $\rho = \frac{b^2}{c}$ is the radius of curvature at the tip of the crack. Note that for cracks with a large aspect ratio, the first term in equation (1) becomes very small relative to the second term. The significance of Inglis' solution is that the high tensile stress necessary for crack propagation will develop at the tips of cracks with large aspect ratios, when the cracks are subject to a remote tensile stress or internal fluid pressure which is only a small fraction of an intact rock's tensile strength.

Griffith's contribution

After Inglis' solution, the second step in understanding crack initiation in rock was Griffith's (1921, 1924) analysis of cracking as a thermodynamic system. A crack subject to high fluid pressure in a rock might have similar properties to a steam piston-cylinder which is capable of expanding against an external force. A steam piston-cylinder consists of one internal component, gas, which is characterized by an equation of state, the ideal gas law. In contrast, a rock consists of two internal components: the crack defined by its long axis, $2c$, and the solid rock defined by its elastic properties (Fig. 3.2). Fluid pressure within the crack, as well as confining pressure on the rock, is equivalent to the load on the piston of the steam cylinder. In the steam piston-cylinder, adiabatic work by the system on the load (F), W is positive.

$$\Delta U_T = -\Delta U_{ST} + W = nRT \int_{V_b}^{V_a} \frac{dV}{V} + F\Delta\ell = 0 \tag{3}$$

where the external force on the loading device (i.e. the piston) is compressive. U_T is the total energy of the system, ΔU_{ST} is the change in internal energy of the steam and ℓ is the displacement of the load, F. In driving a crack within a dry rock, one must subject the outer boundary of the rock to a net pull (i.e. a tensile force), so that the boundary moves outward under tension. In a sense, when the exterior walls of the rock displace there is a decrease in potential energy of the loading device which is any boundary traction that might cause the generation of tensile stress, and as a consequence $dW_R<0$. For example, such a loading situation occurs during the stretching of a rock layer within a thrust sheet in the vicinity of a lateral ramp. The subscript R designates work on surrounding rock across boundaries away from the crack. The work to propagate the crack is positive and defined as the

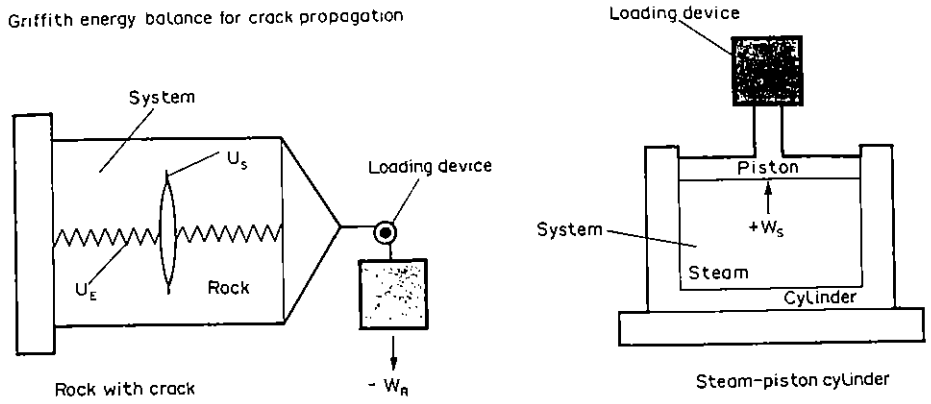

Fig. 3.2. The thermodynamic behaviour of a crack in a rock (after Pollard 1989). See text for details.

increase in surface energy, dU_s. As the crack propagates, the rock will undergo a change in strain energy, dU_E. The total change in energy for crack propagation is

$$\Delta U_T = \Delta U_s - W_R + \Delta U_E. \tag{4}$$

Equation (4) is equivalent to equation (3), but (4) accounts for the complexity of crack propagation. Like the steam piston-cylinder, Griffith (1924) recognized that crack propagation could take place without changing the total energy of the rock-crack system. This is known as the Griffith energy-balance concept where the standard equilibrium requirement is that for an increment of crack extension dc,

$$\frac{dU_T}{dc} = 0. \tag{5}$$

The mechanical and surface energy terms within the rock-crack system must balance over a crack extension, dc. During crack propagation the crack walls move outward to some new lower energy configuration upon removal of the restraining tractions across an increment of crack. In effect, the motion of the crack walls represents a decrease in mechanical energy while work must be expended to remove the restraints across the crack increment. The work to remove the restraints is the surface energy for incremental crack propagation.

To evaluate the three energy terms relating to crack propagation, Griffith cited a theorem of elasticity which states that, for an elastic body under a constant load, the boundaries will displace from the unstressed state to the equilibrium state so that

$$W_R = 2U_E. \tag{6}$$

For a thin plate (i.e. a sheet of rock) containing an elliptical crack with a major axis perpendicular to a uniform tension, Griffith calculated that

$$U_E = \left[\frac{\pi(1-\nu^2)}{E}\right] c^2(\sigma^r)^2 \tag{7}$$

where E is the Young's modulus for the rock and ν is the Poisson ratio. For the surface energy of the crack, Griffith defined crack length as $2c$, and recognized that crack propagation produces two crack faces. Therefore,

$$U_s = 4c\gamma. \tag{8}$$

Substituting equations (6), (7), and (8) into (4) and then applying equation (5), Griffith solved for the critical condition for crack propagation

$$\sigma^r = \left[\frac{2E\gamma}{\pi(1-\nu^2)c}\right]^{1/2}. \tag{9}$$

A crack driven by a tensile traction on an external boundary is one of two end member cases for joint propagation in rocks. The other end member is a crack driven by an internal fluid pressure. In this latter case, the rock is usually in a state of compression from boundary tractions and would, therefore, contain a strain energy due to a compressive external load, σ^r

$$U_E^r = \frac{\pi c^2(\sigma^r)^2}{E}. \tag{10}$$

If the crack is vertical, the vertical, outer boundaries of the local rock-crack system may not displace during crack propagation because the local system is surrounded by adjacent rock-crack systems which are simultaneously attempting to expand. In this case, the rock is in a state of uniaxial strain. If the vertical boundaries do not displace then the rock-crack system does no work against horizontal earth stress during crack propagation, so

$$dW_R = 0. \tag{11a}$$

Therefore, the strain energy term from remote boundary tractions (equation 10) does not enter into Griffith's thermodynamic calculation. In fracture mechanics textbooks this is the 'fixed-grips' case where the loading device does not move the outer boundary of the rock-crack system (e.g. Lawn & Wilshaw 1975).

If we assume that the crack in the rock is internally pressurized but that the pore space behind the crack

remains dry by virtue of an impermeable membrane at the wall of the crack, then we can solve for the crack driving pressure, P_i. When the crack propagates, the crack walls displace, as was the case for crack propagation under tensile boundary tractions. However, in the latter case there was no internal pressure on the crack wall so that no work was done during the displacement of the crack wall. For the case with internal fluid pressure, work is done to move the crack wall by the fluid in the crack

$$dW_c = 2U_E^c \ . \tag{11b}$$

Note that because work was done on the rock-crack system by the crack fluid, the sign of the work term is again negative. Examination of the forces acting on the crack suggest that the crack walls will not part under the influence of P_i until there is a net outward force which happens when $P_i > | \sigma^r |$. The strain energy for movement of the crack wall depends on the net outward force or effective stress within the crack which is the difference between the total stress on the outer boundary of the crack system, σ^r, and fluid pressure inside the crack, P_i,

$$U_E^c = \frac{\pi c^2 (P_i - \sigma^r)^2}{E} \ . \tag{12}$$

We solve equation (6) for the internal pressure necessary to drive the crack when the outer boundary of the rock-crack system is held in a fixed position

$$P_i = \left[\frac{2E\gamma}{\pi(1-\nu^2)c} \right]^{1/2} + \sigma^r \ . \tag{13}$$

This is Secor's (1969) solution to crack propagation under the influence of very high fluid pressures. However, this equation applies only if there is an impermeable membrane between the crack wall and the pore space behind the crack, so that fluid from the crack is not allowed to drain into the pore space. Such a situation is unrealistic.

LINEAR ELASTIC FRACTURE MECHANICS

Conditions defining tensile strength, shear fracturing, and frictional slip on faults are illustrated using the Coulomb–Mohr failure envelope (e.g. Engelder & Marshak 1988, also see Chapters 4 and 5 this volume). Although the Coulomb–Mohr failure envelope serves as a good empirical gauge for the stresses at shear failure, it provides information on neither the rupture path nor post-failure behaviour. Likewise, Griffith's analysis using Inglis' stress concentration factor served well to predict the initiation of crack propagation but proved unsatisfactory as a propagation criterion. This is largely because both the stress field in the vicinity of the crack tip and the radius of the crack tip are poorly defined.

Irwin's contribution

To satisfy the need for a propagation criterion, Irwin (1958) noted that the stress field, σ_{ij}, in the vicinity of a sharp crack tip in an elastic body was approximately proportional to K, the stress intensity factor where

$$\sigma_{ij} \approx \frac{K f_{ij}(\theta)}{(2\pi r)^{1/2}} \ , \tag{14}$$

r and θ are polar coordinates centred at the crack tip. The trigonometric functions, $f_{ij}(\theta)$, vary slightly from unity near the crack tip. These lengthy functions are given in fracture mechanics textbooks (e.g. Broek 1987, Lawn & Wilshaw 1975). Equation (14) for the stress field in the vicinity of the crack tip is remarkable in that the dependence of σ_{ij} on the applied load and geometry of the crack are all incorporated in the stress intensity factor, K. For $r << c$, then $\sigma_{ij} >> \sigma^r$. In general, the equation for K at the crack tip depends on the loading stresses, the length of the crack, $2c$, and the geometry of the body containing the crack which is specified by the dimensionless modification factor, Y,

$$K = Y\sigma^r(c)^{1/2}. \tag{15}$$

For a penny-shaped crack $Y = \frac{2}{\sqrt{\pi}}$, whereas for a tunnel (i.e. blade-shaped) crack $Y = \sqrt{\pi}$. Here a crack will propagate only if the net loading stress is tensile. The engineering literature assigns a positive value to the stress intensity, K, when the net loading stress is tensile. This convention is confusing because it is not consistent with the geological convention of assigning a negative sign to tensile stresses.

Griffith defined the *tensile strength of a rock* in terms of a balance among the work by the loading system, the strain energy within the rock, and the crack surface energy. The tensile strength can also be specified in terms of the critical value of the crack-tip stress intensity at the time of crack propagation

$$K_{Ic} = K \tag{16}$$

where K_{Ic} is called the fracture toughness of the rock. If K_{Ic} is known, then the internal crack fluid pressure necessary to initiate crack propagation is derived from equation (15)

$$P_i = \frac{K_{Ic}}{Y(c)^{1/2}} + \sigma^r \tag{17}$$

where the remote stress is compressive (positive in sign). The net loading stress is actually tensile because $P_i > \sigma^r$. Again this equation assumes that the wall of the crack is impermeable. Experiments on crack propagation have shown that cracks will propagate when $K < K_{Ic}$ at the crack tip (Anderson & Grew 1977, Atkinson 1984). This phenomenon is a process called *subcritical crack growth*. Subcritical crack growth is permitted by

chemical reactions at the crack tip, known as *stress corrosion*, which act to weaken the rock in the vicinity of the tip. Under the influence of stress corrosion, crack propagation may take place at velocities less than 1 mm/s. When cracks propagate under tip stresses equal to K_{Ic}, the cracks travel unstably at speeds which may approach the shear wave velocity of the host rock.

Equation (15) for brittle failure using K_{Ic} should reconcile with Griffith's energy balance (equation 9) (Irwin 1957). If no remote displacements are assumed, the fixed-grips case for crack propagation, then Irwin (1957) showed that the reduction of strain energy in the rock with respect to an increase in crack length is a measure of the energy available for crack propagation

$$G = -\frac{\partial U_E}{\partial c} \tag{18}$$

where G is the energy release rate per unit length of crack tip. For a crack propagating in its own plane G is related to K at the crack tip (Irwin, 1957)

$$G = K^2 \left[\frac{(1-\nu^2)}{E} \right]. \tag{19}$$

The propagation of a crack is resisted by a surface tension force, 2γ, where the cutting of such a crack requires the supply of an amount of energy equivalent to

$$dU_s = 2\gamma dc. \tag{20}$$

For the fixed-grips case where $W_R = 0$, equations (18) and (20) may be substituted into the Griffith energy-balance equation (4)

$$dU_T = -Gdc + 2\gamma dc. \tag{21}$$

At Griffith equilibrium $dU_T = 0$, crack propagation begins when $G = G_c$, so the critical energy release rate is related to the surface energy of the rock

$$G_c = 2\gamma . \tag{22}$$

CRACK PROPAGATION AND PORE PRESSURE

Secor's (1965, 1969) classic model for jointing under the influence of pore pressure postulates that joints initiate from randomly orientated small cracks or flaws which are loaded internally by pore fluid within the rock mass. This form of *fluid-induced joint growth* is akin to fracture propagation during *oil well hydraulic fracturing* (OWHF) and is called *natural hydraulic fracturing* (NHF) (Engelder & Lacazette 1990). There are two important differences between an OWHF and NHF. First, to a rough approximation an OWHF boosts the internal pressure of a borehole (i.e. the initial flaw) without an accompanying increase in pore pressure in the rock behind the borehole wall. Although there is some infiltration through the mudcake on the wall of the borehole, infiltration is confined to the immediate vicinity of the borehole. The mudcake acts like an impermeable membrane. Prior to the initiation of NHF, internal pressure within the initial flaw increases at the same rate as pore pressure in the rock behind the wall of the flaw. For an OWHF a pore pressure increase would decrease breakdown pressure. In contrast, if poroelastic behaviour applies for extension of a penny-shaped flaw during NHF, an increase in pore pressure adds to the load on the crack walls and, in a sense, increases the internal pressure necessary for vertical crack initiation. Second, the crack driving stress for OWHF does not drop abruptly after crack initiation because the borehole is continually charged from surface pumps. In contrast, crack driving stresses for NHF drop either immediately or soon after crack initiation (Secor 1969). Both of these differences impact on our understanding of NHF.

The following are reasons for making the assumption that $P_i = P_p$ at the initiation of NHF. In sedimentary rocks, even with a very low permeability, fluid pressure in one pore will tend to equilibrate with pressure in surrounding pores, provided that the pores are interconnected. There is no known mechanism for suddenly increasing pressure in one pore relative to its neighbours as is the case for an OWHF where $P_i > P_p$. As abnormally high fluid pressures develop in sedimentary basins, pore pressure increases uniformly in the immediate vicinity of the incipient joint, and so the mechanism for the initiation of NHF must operate even though $P_i = P_p$.

The effect of poroelasticity

Price (in Fyfe *et al.* 1978) and more recently Gretener (1981) have correctly pointed out that Secor's model neglects the role of pore pressure (i.e. poroelasticity) in increasing the total stress on the crack wall. Although Fyfe *et al.* (1978) appear to recognize that Secor's (1965) mechanism is viable if the general law of effective stress (Nur & Byerlee 1971) is used in place of the simple law, their analysis needs clarification (Engelder & Lacazette 1990).

The poroelastic effect is visualized using a force-balance model (Fig. 3.3). Grain boundaries are characterized by the elastic grain–grain contacts and pore space between the grains. All the pores are connected so that the aggregate has a relatively high permeability. An initial flaw or small crack is introduced into the aggregate by a cut through the centre of the model. Two halves of the aggregate are compressed together in a container with rigid walls. Initially the aggregate is dry so that the rigid walls of the container press the initial flaw together with an average force per unit area, S_t. S_t represents a rock stress normal to the flaw. The aggregate is then filled with a pore fluid at a relatively low pressure P_p. If the face of the initial

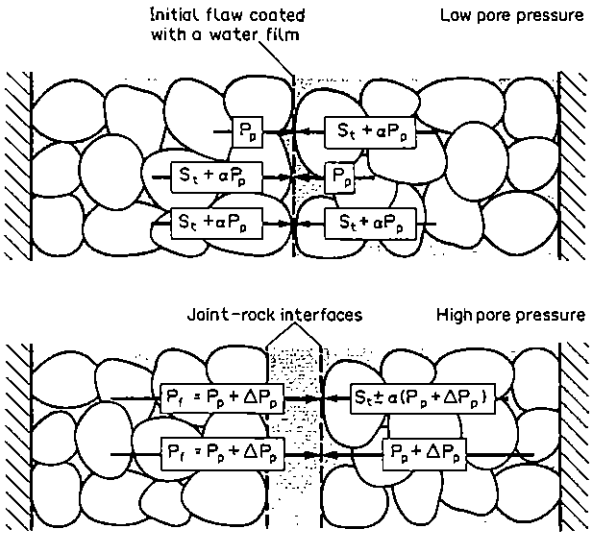

Fig. 3.3. Poroelastic model for a rock with an initial flaw and constrained by rigid boundaries on all sides. The model consists of grains, elastic grain–grain contacts, and interconnected pore space. Vectors are shown to represent the balance of forces along the initial flaw interface and the joint-rock interface. Symbols explained in text.

flaw is considered as an impermeable interface, the addition of pore fluid within the flaw would cause a uniform increase in the stress along the interface, yet the addition of pore fluid within the aggregate would not cause a uniform increase in stress from the aggregate side of the interface. Where pore fluid was in direct contact with the interface from the aggregate side, the pressure on the interface would increase by P_p. Where grains were in contact with the interface the normal stress on the interface would increase by a fraction, α, of P_p. This fractional increase in normal stress arises because the grain contacts are cemented and act like springs which take-up part of the force exerted by pore fluid inside pores. This partial transfer of pore pressure to the aggregate boundary is known as the *poroelastic effect* (Biot 1941). Without an impermeable interface, any increase in P_p within the initial flaw will act to open the initial flaw, but this increase is partially counterbalanced by a poroelastic expansion within the aggregate which acts to keep the initial flaw closed.

Too initiate crack propagation for both OWHF and NHF, internal fluid pressure must counterbalance the total least principal stress, σ_3 (i.e. $S_t + \alpha P_p$ in the model shown in Fig. 3.3). Poroelastic behaviour applies to the development of vertical joints, where the total least horizontal stress, S_h is equal to σ_3. In saturated rocks, total stress may be divided into two components: the stress carried by grain–grain contacts under dry conditions (i.e. S_t in Fig. 3.3) and stress generated by fluid pressure within the pore space of the rock (i.e. αP_p in Fig. 3.3). By the poroelastic effect an increase in P_p will cause an increase in total stress provided that the rock is constrained by rigid boundaries. One type of rigid boundary behaviour is called *uniaxial strain* which is a common model for horizontal strain in sedimentary basins (Geertsma 1957):

$$\varepsilon_H = \varepsilon_h = 0, \tag{23a}$$

$$\varepsilon_v \neq 0 \tag{23b}$$

ε_H and ε_h are principal strains in the horizontal direction. The effect of a change in pore pressure in sedimentary basins may be seen by solving Biot's (1941) elasticity equations for uniaxial strain. Biot's elasticity equations are given by Rice & Cleary (1976) as

$$2\,\Gamma\varepsilon_{ij} = \langle\,\sigma_{ij}\,\rangle - \frac{\nu}{1+\nu}\langle\,\sigma_{kk}\,\rangle\,\delta_{ij} \tag{24a}$$

where

$$\langle\,\sigma_{ij}\,\rangle = \sigma_{ij} + \alpha P_p\ . \tag{24b}$$

In Biot's equations, α is Biot's poroelastic term defined as $\{1 - C_i/C_b\}$ with the intrinsic compressibility of the uncracked solid, C_i (i.e. the compressibility of the solid grains in Fig. 3.2), and the bulk compressibility of the solid with cracks and pores, C_b (i.e. the compressibility controlled largely by the 'springs' in Fig. 3.3) (Nur & Byerlee 1971). Γ and ν are the shear modulus and Poisson ratio of the rock when it is deformed under 'drained' conditions.

For this analysis of vertical joints and veins, the crack-normal stress is the least horizontal stress, S_h. Little is known about the least horizontal stress in a sedimentary basin where vertical joints are forming except the obvious; the total horizontal stress, $S_h < S_v$. The total vertical stress is

$$S_v = \rho_t g z \tag{25}$$

where ρ_t is the integrated density of the rock to the depth, z, of interest and g is the acceleration of gravity. Although the state of stress was probably more complicated, I make the simplifying assumption that S_h was equal to that found in a tectonically relaxed basin.

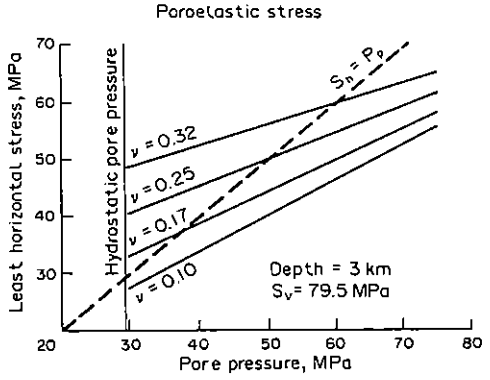

Fig. 3.4. Relationship between S_h and P_p in a tectonically relaxed basin assuming poroelastic behaviour. In a tectonically relaxed basin, horizontal stresses are due solely to the overburden load. The poroelastic effect is strongly dependent on Poisson's ratio, ν, as indicated by the four curves for various values of ν. This calculation assumes conditions at a depth of burial of 3 km.

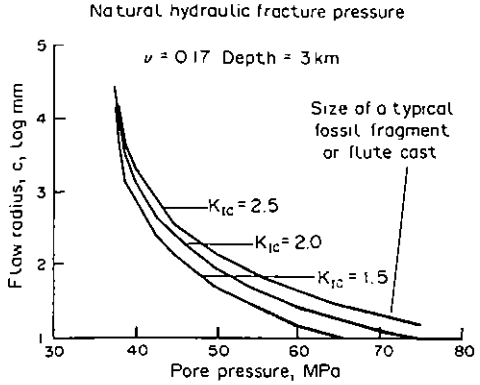

Fig. 3.5. Relationship between flaw or crack length and pore pressure required to initiate cross-fold joint propagation in a tectonically relaxed basin assuming poroelastic behaviour. The flaw length at initiation of propagation is moderately dependent on the K_{Ic} of the rocks within which crack propagation takes place. This calculation assumes a penny-shaped flaw, a burial depth of 3 km and a ν of 0.17 for a siltstone.

A tectonically relaxed basin is one in which S_h is proportional to S_v through the uniaxial elastic strain model:

$$S_h = \frac{\nu}{1-\nu} S_v \ . \tag{26}$$

Solving Biot's elasticity equations for uniaxial strain

$$S_h = \frac{\nu}{1-\nu} S_v + \frac{(1-2\nu)}{(1-\nu)} \alpha P_p \ . \tag{27a}$$

Terms in this equation may be rearranged to appear in the same form as equation (13) derived by Anderson *et al.* (1973) for fracture pressure at a borehole

$$S_h = \frac{\nu}{1-\nu} (S_v - \alpha P_p) + \alpha P_p \ . \tag{27b}$$

The first term on the right-hand side of equation (27b) is equivalent to but not the same as S_t in Fig. 3.3.

The internal fluid pressure, P_i, necessary to initiate crack propagation and thereby cause NHF is a function of several general parameters including total rock stress normal to the crack plane, S_h, and the elastic properties of the rock. To understand the variation of P_i, it is appropriate to consider the variation of S_h due to the poroelastic effect in a tectonically relaxed basin (Fig. 3.4). The calculations for Fig. 3.4 assume 3 km of overburden having a density of 2.7 g/cc so that S_v = 79.5 MPa. An α of 0.7 is also assumed. S_h can vary by as much as 50% of the overburden weight depending on ν and P_p. A larger S_h is generated in rock with a higher ν. The field of interest in Fig. 3.4 is defined by $P_p > S_h$ for it is within this field that NHF occurs. In rocks with a very low ν, conditions favouring NHF occur even at hydrostatic pore pressure whereas for rocks with a high ν, conditions for NHF are suppressed until a much higher P_p.

The initiation of NHF

For several reasons it is not intuitively obvious that a net tensile stress (i.e. a crack driving stress) is generated along an initial flaw: (1) a compressive stress, S_h, increases as a function of P_p, (2) pores of the rock behind the flaw are also subject to the same pressure, and (3) fluids can readily drain from the flaw to the pore space. The poroelastic behaviour of rock, for which $\alpha < 1$, is responsible for the generation of a net tensile stress against the face of a flaw.

In addition to total rock stress, the internal fluid pressure, P_i necessary to initiate joint propagation is a function of the fracture toughness of the rock, K_{Ic}, the crack length, $2c$, and the shape of the crack, Y. K_I, a measure of the stress concentration at a crack tip, increases with an increase in net tensile stress on the crack. K_{Ic}, the *critical stress intensity factor* or *fracture toughness* is a material property that indicates the ease with which a rock will fracture. K_{Ic} is a laboratory measure of the pull normal to a crack plane at the time the crack tip propagates rapidly. *Joint initiation* occurs only when the crack (i.e. initial flaw) walls are pulled apart or subject to a net tensile stress as a consequence of the poroelastic effect. The linear elastic fracture mechanics equation for the rapid growth of a joint is

$$P_i = \left\{ \frac{K_{Ic}}{Yc^{1/2}} \right\} . \tag{28a}$$

This is the condition if the walls of the crack are not supported by an earth stress. If the walls of the crack are forced closed by S_h, then

$$P_i = \left\{ \frac{K_{Ic}}{Yc^{1/2}} \right\} + \frac{\nu}{1-\nu} S_v + \frac{(1-2\nu)}{(1-\nu)} \alpha P_p \ . \tag{28b}$$

As equation (28b) indicates, P_i can vary significantly depending on the size of the pre-existing crack. In Fig. 3.3 the difference between the length of the vector for normal stress across a grain and the vector for fluid pressure is the vector for $K_{Ic}/Yc^{1/2}$.

The equations developed above may be used in conjunction with measured rock properties to constrain the stress and pore conditions under which a given set of natural hydraulic fractures initiated. Under the assumption that joints formed by NHF started propagating rapidly from small cracks or flaws when $P_i = P_p$, equation (28b) may be rewritten to give an indication of flaw length leading to initiation of joints.

$$c = \left[\frac{K_{Ic}}{Y\left\{ P_i - \frac{\nu}{1-\nu} S_v - \frac{(1-2\nu)}{1-\nu)} \alpha P_p \right\}} \right]^2 . \tag{29}$$

To illustrate the initiation and propagation of joints under high fluid pressures, the properties of a siltstone from the Appalachian Plateau are used (Engelder & Lacazette 1990). Typically K_{Ic} of rocks varies between 2.5 MPam$^{1/2}$ and 1.5 MPam$^{1/2}$ (Atkinson 1984).

Laboratory measurements of ν for siltstones of the Appalachian Plateau suggest that $\nu = 0.17$ is reasonable (Evans *et al.* 1989). All flaws in the siltstone are assumed to be penny-shaped cracks which have $Y = 1.13$. Using equation (29) the flaw radius for NHF initiation within the siltstone varies as a function of pore pressure at a depth of 3 km. These calculations assume three arbitrary values of K_{Ic} for joint initiation (2.5, 2.0, and 1.5 MPam$^{1/2}$). (Fig. 3.5). Figure 3.5 shows that joints will initiate from larger flaws at lower P_p.

At an early stage in their development rocks have no large joints but contain either microcracks in the form of pore space and grain boundaries, or flaws in the form of fossil and/or rock fragments and sedimentary structures such as flute casts. Unfractured siltstone has two types of flaws: grain boundary microcracks and larger structures such as flute casts, concretions, and fossil fragments. Grain-boundary microcracks are on the scale of individual grains less than 0.1 mm in diameter. In contrast, fossil fragments and flute casts are roughly 1 – 3 cm in diameter. The plumose surface morphology on the surface of cross-fold joints in the siltstone from the Appalachian Plateau allows the joint propagation to be traced back to origin flaws which are commonly 1 – 3 cm structures. From this observation in flaw size, $2c$, is known for the initiation of NHF. Assuming conditions in a tectonically relaxed basin at a depth of 3 km, pore pressure at the initiation of NHF was on the order of 65 MPa or higher.

Figures 3.5 and 3.6 illustrate several points concerning the effect of both ν and K_{Ic} on the flaw length for the initiation of joints. First, grain boundary microcracks are too small to account for the initial propagation of NHF, even if siltstones have an extremely low ν. Second, abnormal pore pressures, significantly above hydrostatic, were necessary for the initiation of joints at depth. Third, at $\nu = 0.17$, typical fossil fragments or flute casts were large enough flaws

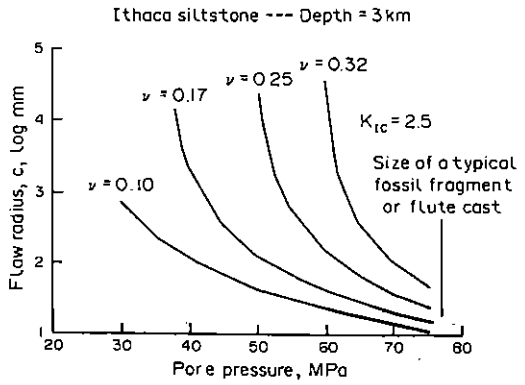

Fig. 3.6. Relationship between flaw or crack length and pore pressure required to initiate crack propagation within a siltstone. The flaw length at initiation of cross-fold joints is strongly dependent on the Poisson's ratio (ν) of the rocks within which crack propagation takes place. This calculation assumes a penny-shaped flaw, a tectonically relaxed basin with a poroelastic response to changes in pore pressure, a burial depth of 3 km, and a K_{Ic} of 2.5 MPam$^{1/2}$ for a siltstone.

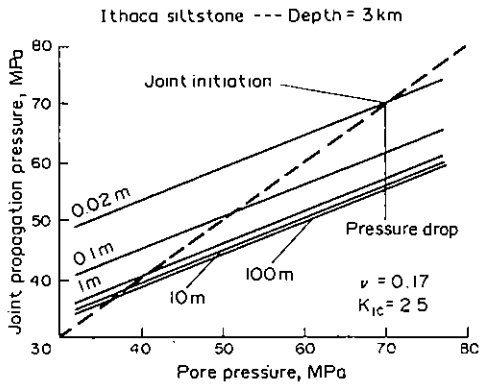

Fig. 3.7. Relationship between crack propagation pressure and pore pressure for cross-fold joints of lengths between 0.02 and 100 m. This calculation assumes a tunnel crack, a burial depth of 3 km, a K_{Ic} of 2.5 MPam$^{1/2}$, and a ν of 0.17 for a siltstone. See text for details.

to favour the initiation of vertical joints at 3 km. Fourth, in a bedded siltstone – shale sequence, the initiation of NHF is favoured in a rock with a lower ν (i.e. a siltstone) relative to a rock with higher ν (i.e. a shale).

Once joints have initiated from small flaws, less severe internal pressures are necessary for further growth. Equation (29) also gives the incremental crack propagation pressure. Suppose that a vertical joint initiates from an initial flaw with a radius of about 1 cm. At initiation $P_p = P_i = 68$ MPa (Fig. 3.5). By the time a joint has run to a length of 30 cm, an internal pressure 20 MP less than P_p is required for reinitiation of joint propagation. Reinitiation pressure decreases to approach the total stress normal to the crack wall. Figure 3.7 illustrates the difference between crack initiation pressure and crack propagation pressure. Crack initiation pressure is indicated by the dashed line cutting across the propagation pressure – pore pressure lines for joints of various lengths. Once a joint propagates to a length of more than one metre, the crack propagation pressure changes very little. However, that pressure may be more than 20 MPa less than the crack initiation pressure.

OTHER DETAILS OF THE MECHANICS OF JOINTING

Joint-propagation path

The *joint-propagation path* is that direction which the rupture takes as it leaves the present *joint front or tip* of the crack. The joint-tip stress field, as given in equation (14), controls the joint propagation path at the joint front. One method for charting the crack path through a rock is to consider the stress intensity for small increments of growth. To a first approximation, the crack will propagate in a direction normal to the least principal stress. This is the orientation which will produce the maximum propagation energy, G (Pollard

& Aydin 1988). If the crack is subject to pure opening mode loading (i.e. stress normal to the crack plane on a *Mode I* crack) each increment of crack propagation will be in the plane of the initial crack. As long as the orientation of the extensional stress field does not change at the tip of the crack a planar joint is produced. If the crack is subject to a shear couple, then each propagation increment will turn and the crack will continue in a path so that the subsequent crack plane is normal to the extension direction. Such a turn is known as out-of-plane propagation of which there are two types, a twist and a tilt. A *tilt* is a turn of the crack rupture about an axis parallel to the joint front and this occurs when the crack is subject to *Mode 2* loading. A *twist* takes place as the joint front turns about an axis perpendicular to the joint front. During a tilt the joint maintains its continuity but during a twist the joint breaks into en échelon segments.

Joint arrest

Joint arrest is best modelled by considering the energy release rate per unit crack propagation, G (equation 19). The energy release rate is proportional to the driving stress and the square root of the crack length. There is a critical value of G for which crack propagation will take place, G_c. Some authors call this critical rate the *crack growth resistance, R* (Broek 1987). Once $G = G_c$, the crack will continue to propagate unless the driving stress decreases. In the case of a fluid driven crack the volume increase of the crack is proportional to the crack opening displacement or COD

$$\text{COD} = \frac{4\sigma(1-\nu^2)c}{E}. \qquad (30)$$

As the volume of the crack increases with crack tip displacement the pressure of the fluid within the crack must decrease as indicated by the equation of state of the fluid. Propagation will arrest once the driving pressure has dropped, so that G is less than R.

Mechanical interaction

A very common outcrop pattern consists of two joints overlapping each other slightly. Each joint is planar until the joints approach closely, at which point the joints may tend to diverge and then rotate sharply toward each other. This pattern reflects the mechanical interaction between joints as their tips propagate toward each other. As joint tips approach, each joint induces a tensile stress in the vicinity of its neighbour's tip and therefore enhances the propagation energy of the neighbour. At the same time each joint induces a shear stress in the neighbour's propagation plane. This shear stress will at first cause the neighbours to deflect away from each other. As the en échelon joints pass, each joint induces a compressive stress field with shear stress oriented so that the joints will then propagate toward each other (also see Chapter 5).

This same type of mechanical interaction is seen for joints of different lengths which are completely overlapping. A longer joint will shield the shorter joint from the overall tensile stress field which is driving the joint. As the length of the longer joint increases the tensile stress on the neighbouring shorter joint decreases by this shielding effect. In an outcrop of many joints a few long joints will prevent the extension of many neighbouring shorter joints. This mechanical interaction is largely responsible for joint spacing within rocks.

CONCLUSIONS

Recent advances in the understanding of brittle deformation processes include the application of linear elastic fracture mechanics to geological problems. This review illustrated this application with examples concerning the effect of high fluid pressure on crack propagation in rocks.

Acknowledgements — This paper was written in conjunction with support from the Gas Research Institute under contract # 5088-260-1746. Alfred Lacazette is thanked for his review of an early version of this paper.

REFERENCES

Anderson, O. L. & Grew, P. C. 1977. Stress corrosion theory of crack propagation with applications to geophysics. *Rev. Geophys. Space Phys.* **15**, 77 – 104.

Anderson, R. A., Ingram, D. S. & Zanier, A. M. 1973. Determining fracture pressure gradients from well logs. *J. Petrol. Technol.* **26**, 1259 – 1268.

Atkinson, B. K. 1984. Subcritical crack growth in geological materials. *J. geophys. Res.* **89**, 4077 – 4114.

Atkinson, B. K. (ed.) 1987. *Fracture Mechanics of Rock.* Academic Press, Orlando.

Badgley, P. C. 1965. *Structural and Tectonic Principals*, Harper & Row, New York.

Biot, M. A. 1941. General theory of three-dimensional consolidation. *J. appl. Phys.* **12**, 155 – 164.

Brace, W. F. & Bombolakis, E. G. 1963. A note on brittle crack growth in compression. *J. geophys. Res.* **68**, 3709 – 3713.

Brace, W. F. & Kohlstedt, D. L. 1980. Limits on lithospheric stress imposed by laboratory experiments. *J. geophys. Res.* **85**, 6248 – 6252.

Broek, D. 1987. *Elementary Engineering Fracture Mechanics.* Martinus Nijhoff, Dordrecht, The Netherlands.

Bucher, W. H. 1920. The mechanical interpretation of joints. *J. Geol.* **28**, 707 – 730.

Byerlee, J. 1978. Friction in rocks. *Pure appl. Geophys.* **116**, 615 – 626.

Engelder, T. 1982. Is there a genetic relationship between selected regional joints and contemporary stress within the lithosphere of North America? *Tectonics* **1**, 161 – 177.

Engelder, T. & Lacazette, A. 1990. Natural hydraulic fracturing. In *Rock Joints* (edited by Barton, N. & Stephansson, O.). A. A. Balkema, Rotterdam, 35 – 44.

Engelder, T. & Marshak, S. 1988. The analysis of data from rock-deformation experiments. In: *Basic Methods of Structural Geology* (edited by Marshak, S. & Mitra, G.). Prentice-Hall, Englewood Cliffs, 193 – 212.

Etheridge, M. A. 1983. Differential stress magnitudes during regional deformation and metamorphism: upper bound imposed by tensile fracturing. *Geology* **11**, 231 – 234.

Evans, K., Oertel, G. & Engelder, T. 1989. Appalachian Stress Study 2: Analysis of Devonian shale core: Some implications for the nature of contemporary stress variations and Alleghanian deformation in Devonian rocks. *J. geophys. Res.* **94**, 7155 – 7170.

Fyfe, W. S., Price, N. J. & Thompson, A. B. 1978. *Fluids in the Earth's Crust*. Elsevier, New York.

Gallagher, J. J., Friedman, M., Handin, J. & Sowers, G. 1974. Experimental studies relating to microfracture in sandstone. *Tectonophysics* **21**, 203 – 247.

Geertsma, J. 1957. The effect of fluid pressure decline on volumetric changes of porous rock. *Trans. AIME* **210**, 331 – 339.

Griffith, A. A. 1920. The phenomena of rupture and flow in solids. *Phil. Trans. R. Soc. Lond.* **A221**, 163.

Griffith, A. A. 1924. Theory of rupture. *Proc. First Int. Cong. appl. Mech. Delft*, 55 – 63.

Gretener, P. E. 1981. *Pore Pressure: Fundamentals, General Ramifications, and Implications for Structural Geology*. American Association of Petroleum Geologists Educational Course Note Series **4**, 1 – 131.

Hancock, P. L. & Engelder, T. 1989. Neotectonic Joints. *Geol. Soc. Am. Bull.* **101**, 1197 – 1208.

Handin, J. & Hager, R. V. 1957. Experimental deformation of sedimentary rocks under confining pressure: tests at room temperature on dry samples. *Bull. Am. Assoc. Petrol. Geol.* **41**, 1 – 50.

Inglis, C. E. 1913. Stresses in a plate due to the presence of cracks and sharp corners. *Trans. Inst. Naval. Archit.* **55**, 219.

Irwin, G. R. 1957. Analysis of stress and strains near the end of a crack traversing a plate. *J. appl. Mech.* **24**, 361 – 364.

Lawn, B. R. & Wilshaw, T. R. 1975. *Fracture of Brittle Solids*. Cambridge University Press, Cambridge.

McClintock, F. A. & Walsh, J. B. 1962. Friction of Griffith cracks under pressure. *4th U.S. nat. Cong. appl. Mech. Proc.*, 1015 – 1021.

Nickelsen, R. P. & Hough, V. D. 1967. Jointing in the Appalachian Plateau of Pennsylvania. *Bull. geol. Soc. Am.* **78**, 609 – 630.

Nur, A. & Byerlee, J. D. 1971. An exact effective stress law for elastic deformation of rocks with fluids. *J. geophys. Res.* **76**, 6414 – 6419.

Pollard, D. D. & Aydin, A. 1988. Progress in understanding jointing over the past century. *Bull. geol. Soc. Am.* **100**, 1181 – 1204.

Rice, J. R. & Cleary, M. P. 1976. Some basic diffusion solutions for fluid-saturated elastic porous media with compressible constituents. *Rev. Geophys. Space Phys.* **14**, 227 – 241.

Rossmanith, H. P. (ed.) 1983. *Rock Fracture Mechanics*. Springer, New York.

Scheidegger, A. E. 1982. Comment on "Is there a genetic relationship between selected regional joints and contemporary stress within the lithosphere of North America?" by T. Engelder. *Tectonics* **1**, 463 – 464.

Scholz, C. H. 1968. Microfacturing and the inelastic deformation of rock in compression. *J. geophys. Res.* **73**, 1417 – 1432.

Secor, D. T. 1965. Role of fluid pressure in jointing. *Am. J. Sci.* **263**, 633 – 646.

Secor, D. T. 1968. Mechanics of natural extension fracturing at depth in the earth's crust. *Geol. Surv. Pap. Can.* **68 – 52**, 3 – 48.

Voight, B. & St. Pierre, B. H. P. 1974. Stress history and rock stress. *Adv. Rock Mech. Proc 3rd Cong. ISRM* **II**, 580 – 582.